Contribution from the Department of Chemistry and NMR Facility, University of California, Davis, California 95616

Assignment by 2D NMR Bond Correlation Spectroscopy of Hyperfine-Shifted and Strongly Relaxed Protons in Iron Porphyrin and Chlorin Complexes

Kelly A. Keating,† Jeffrey S. de Ropp,‡ Gerd N. La Mar,*,† Alan L. Balch,† Fuu-Yau Shiau,† and Kevin M. Smith†

Received January 30, 1991

Two-dimensional magnitude COSY experiments have been carried out on a variety of paramagnetic iron complexes of porphyrins and chlorins, including the ferric low-spin and both ferric and ferrous high-spin states. Numerous cross peaks that reflect spin connectivity between resonances with line widths to 150 Hz are clearly detectable. For low-spin ferric complexes of pyropheophorbide *a*, essentially all spin connectivities that would be found in a diamagnetic analogue are observed. In the high-spin ferric complexes of both protoporphyrin IX and pyropheophorbide *a*, COSY cross peaks provide assignments for pairs of protons with expected coupling constants >5 Hz. While the cross-peak intensities in the high-spin ferric complexes are strongly diminished relative to low-spin ferric systems due to both relaxation and antiphase cancellation, the repetition rates of the experiment can be significantly increased due to the shorter relaxation times. This compensation allows the detection of cross peaks within a reasonable time. In the high-spin ferrous complexes of *N*-methylporphines, the COSY data indicate that the spin density distribution is as asymmetric within a pyrrole as it is between the nonequivalent pyrroles. The surprising success of magnitude COSY experiments with the "worst case scenario" high-spin ferric systems indicates that 2D COSY can be routinely incorporated into the assignment strategies for paramagnetic iron tetrapyrrole complexes.

Introduction

The proton NMR spectra of paramagnetic transition-metal complexes yield valuable information on magnetic and electronic properties of the metal center, as well as on the nature and extent of metal–ligand covalency.[1,2] The iron complexes of the cyclic tetrapyrroles, the porphyrins and chlorins, are a particularly important group of complexes. All but one of the commonly accessible oxidation/spin states are paramagnetic, and the detailed patterns of the hyperfine shifts for the tetrapyrrole have been shown to be essentially diagnostic for a given oxidation/spin/ligation state of the iron.[3-5] The close parallel between hyperfine shift patterns of iron tetrapyrrole complexes and the intact hemoproteins[4,6] with the same chromophore[4] has made the simple complexes ideal models for elucidating protein-based spectral perturbations in the latter systems. Moreover, the asymmetric functionalization of the tetrapyrrole periphery leads to redistribution of the delocalized spin density that provides us with one of the most sensitive methods for mapping ligand molecular orbitals.[7-9] The most serious barrier to the full utilization of the NMR spectral information in paramagnetic model complexes is the unambiguous assignment of the resonances, since the hyperfine shifts invalidate the functional group/shift correlation of diamagnetic systems and generally paramagnetic relaxation obscures multiplet structure.

Initially, the assignment strategies have relied on difficult isotope labeling and analysis of differential paramagnetic induced relaxation in terms of distance from the metal. One of the shortcomings of isotope labeling is that it is frequently only possible to deuterate collectively a set of similar but not identical functional groups.[8-10] Assignments based solely on relaxation influences are undependable because of relaxation by delocalized spin density.[11,12] More recently, 1D nuclear Overhauser effect,[13] NOE, measurements have been used to identify spatial proximity of protons in model hemes[14] and chlorins,[15,16] particularly in cases where the complex is immobilized in a viscous solvent.[14,17] In one case, a complete NOESY map could be obtained[17] for a low-spin ferric heme with only weak paramagnetic relaxation. However, even the NOE-based assignments indicate only spatial proximity from which the nature of functional groups must be inferred. The functional groups, as in the case of proteins, are ideally identified by their unique spin–spin connectivity patterns.

Considerably less attention[18,19] has been directed toward 2D bond correlation experiments for resonance assignment. These detect the characteristic spin (scalar) connectivity[20,21] of peripheral substituents of tetrapyrrole complexes. This neglect is likely due to the belief that the severe line broadening that can accompany paramagnetism obscures the multiplet structure and renders the detection of coherence in a COSY map experimentally impossible. The evolution in time, t, of the coherence responsible for the cross peaks, a_{ij}, between two spin-coupled protons i, j with coupling constant J_{ij} is given by[20,21]

$$a_{ij} = [\sin(\pi J_{ij} t)] e^{-t/T_2} \quad (1)$$

where T_2 is the spin–spin relaxation time related to the line width, Δ, via $T_2 = (\pi\Delta)^{-1}$. For a strongly relaxed line, $T_2^{-1} > J$, and the decay (second) term in eq 1 competes effectively with the development of coherence (first term in eq 1). However, for

† Department of Chemistry.
‡ NMR Facility.

(1) La Mar, G. N., Horrocks, Jr., W. D., Holm, R. H., Eds. *NMR of Paramagnetic Molecules*; Academic Press: New York, 1973.
(2) Bertini, I.; Luchinat, C. *NMR of Paramagnetic Molecules in Biological Systems*; Benjamin/Cummings: Menlo Park, CA, 1986.
(3) La Mar, G. N.; Walker, F. A. *The Porphyrins*; Academic Press: New York, 1979; Vol. 4, p 61.
(4) La Mar, G. N. In *Biological Applications of Magnetic Resonance*; Shulman, R. G., Ed.; Academic Press: New York, 1979; p 305.
(5) Latos-Grazynski, L.; Balch, A. L.; La Mar, G. N. *Adv. Chem. Ser.* **1982**, *No. 201*, 661.
(6) Satterlee, J. D. *Annu. Rep. NMR Spectrosc.* **1986**, *17*, 79.
(7) La Mar, G. N.; Viscio, D. B.; Smith, K. M.; Caughey, W. S.; Smith, M. L. *J. Am. Chem. Soc.* **1978**, *100*, 8085.
(8) Latos-Grazynski, L.; Cheng, R.-J.; La Mar, G. N.; Balch, A. L. *J. Am. Chem. Soc.* **1981**, *103*, 4270.
(9) Balch, A. L.; Chan, Y.-W.; La Mar, G. N.; Latos-Grazynski, L.; Renner, M. W. *Inorg. Chem.* **1985**, *24*, 1437.
(10) Budd, D. L.; La Mar, G. N.; Langry, K. C.; Smith, K. M.; Nayyir-Mazhir, R. *J. Am. Chem. Soc.* **1979**, *101*, 6091.
(11) Unger, S. W.; Jue, T.; La Mar, G. N. *J. Magn. Reson.* **1985**, *61*, 448.
(12) Arasasingham, R. D.; Balch, A. L.; Cornman, C. R.; de Ropp, J. S.; Eguchi, K.; La Mar, G. N. *Inorg. Chem.* **1990**, *29*, 1847.
(13) Neuhaus, D.; Williamson, M. *The Nuclear Overhauser Effect in Structural and Conformational Analysis*; VCH Publishers: New York, 1989.
(14) Yu, C.; Unger, S. W.; La Mar, G. N. *J. Magn. Reson.* **1986**, *67*, 346.
(15) Chatfield, M. J.; La Mar, G. N.; Parker, Jr., W. O.; Smith, K. M.; Leung, H.-K.; Morris, I. K. *J. Am. Chem. Soc.* **1988**, *110*, 6352.
(16) Licoccia, S.; Chatfield, M. J.; La Mar, G. N.; Smith, K. M.; Mansfield, K. E.; Anderson, R. R. *J. Am. Chem. Soc.* **1989**, *111*, 6087.
(17) Dugad, L. B.; La Mar, G. N.; Unger, S. W. *J. Am. Chem. Soc.* **1990**, *112*, 1386.
(18) Peters, W.; Fuchs, M.; Sicius, H.; Kuchen, W. *Angew. Chem., Int. Ed. Engl.* **1985**, *24*, 231.
(19) Jenkins, B. G.; Lauffer, R. B. *J. Magn. Reson.* **1988**, *80*, 328.
(20) Martin, G. E.; Zektzer, A. S. *Two-Dimensional NMR Methods for Establishing Molecular Connectivity*; VCH Publishers: New York, 1988.
(21) Ernst, R. R.; Bodenhausen, G.; Wokaun, A. *Principles of Nuclear Magnetic Resonance in One and Two Dimensions*; Clarendon Press: Oxford, England, 1987; Chapter 8.

0020-1669/91/1330-3258$02.50/0

Chart I

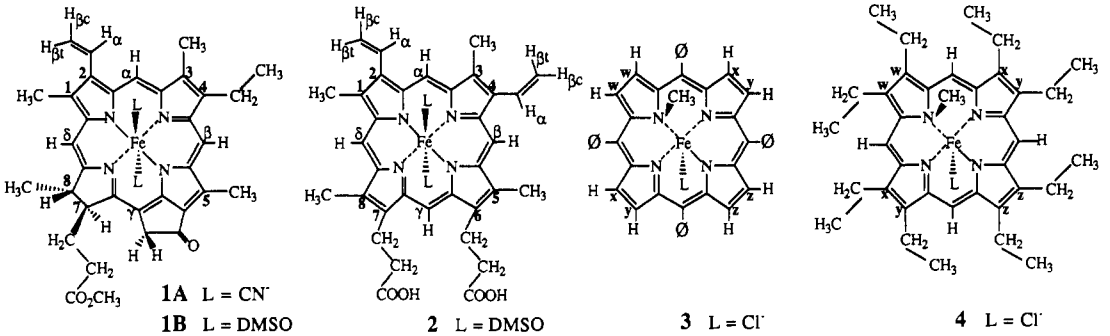

1A L = CN^- **1B** L = DMSO **2** L = DMSO **3** L = Cl^- **4** L = Cl^-

nonzero J and finite T_2, coherence, however weak and short-lived, does exist. The detection of the weak coherence is further thwarted by the fact that COSY cross peaks exhibit antiphase properties,[20,21] which has the result of causing cancellation of the detectable coherence. This latter effect is exacerbated as line width increases at fixed J or J decreases for fixed line width.

In order to evaluate the likely impact of 2D spin connectivity experiments on assignment strategies for paramagnetic complexes, we target here iron porphyrin and chlorin complexes in a variety of oxidation/spin states that range from the low-spin ferric state with well-resolved lines that exhibit some multiplet structure[3,4,7,15,16] to the "worst case scenario" high-spin ferric complexes, which exhibit the broadest lines.[3-5,10,16] The structures of the complexes of the particular macrocycles of interest, **1–4**, are given in Chart I. All of these complexes have been previously investigated by 1D ^{1}H NMR spectroscopy.[8,10,16] The spectrum of the low-spin bis(cyano) complex of (pyropheophorbidato *a*)iron(III) (**1A**) has been completely assigned[16] by a combination of spin decoupling and 1D NOEs. The ^{1}H NMR spectra of the four high-spin complexes bis(dimethyl sulfoxide)(protoporphyrinato IX)iron(III) (**2**), bis(dimethyl sulfoxide)(pyropheophorbidato *a*)iron(III) (**1B**), (*N*-methyltetraphenylporphyrinato)iron(II) chloride (**3**), and (*N*-methyloctaethylporphyrinato)iron(II) chloride (**4**) have been reported[9,10,16] and partial collective assignments determined by limited selective deuteration. These complexes are representative of extremes in line width, T_1, and chemical shift dispersion encountered in such model complexes[3-5] and serve as severe tests of the scope and limitations of 2D bond correlation experiments. At the same time, these complexes have several unanswered questions as to their detailed electronic structure that could be addressed with the aid of an effective assignment strategy. Previous 2D NMR studies of low-spin ferric myoglobin have revealed[22] that, of the various spin connectivity experiments,[20,21,23] magnitude COSY, MCOSY,[23,24] is the most effective variant of the 2D bond correlation experiments for detecting cross peaks between rapidly relaxed resonances. For the pertinent case where $T_2^{-1} \gg J$, optimal detection of cross peaks balances the cross-peak buildup, i.e., sin (πJt), against the decay, i.e., e^{-t/T_2}, which is achieved with an acquisition time in both dimensions equal to $2T_2$ for the broader of the two spin-coupled lines of interest and apodization over $2T_2$ of the signal with a pseudoecho filter such as 0°-shifted sine-bell or sine-bell-squared window.[23]

Experimental Section

Samples were prepared as described in detail previously[9,10,16] and consisted of 3–10 mM complex in the appropriate deuterated solvent. ^{1}H NMR spectra were collected on General Electric Ω-300 and Ω-500 spectrometers operating in quadrature mode at 300 and 500 MHz, respectively. All 1D reference spectra were collected by using a standard one-pulse experiment, with a presaturation pulse when necessary to suppress the solvent signal, and with a $5T_1$ interpulse delay. Nonselective T_1s were obtained from the initial slope of the semilogarithmic plots of the intensity data from an inversion-recovery experiment. T_2 values were determined from line width at half-height via $T_2 = (\pi\Delta)^{-1}$. For 2D spectra, an n-type magnitude COSY,[23,24] MCOSY, sequence was used, with a presaturation pulse during the relaxation delay to suppress the solvent resonance when necessary. The 90° pulse lengths were 5–6 μs at 300 MHz and 12 μs at 500 MHz. 2D spectra were collected with either 512 or 1024 points in t_2 over the minimum bandwidth necessary to include all peaks with expected spin connectivities and centered about the solvent resonance when possible. The number of t_2 data points were chosen with the consideration of needing at least $2T_2$ ms for acquisition time length, where T_2 is the longest T_2 value for the complex as estimated from the linewidth for all peaks in the 1D reference spectrum. Resulting acquisition times for the spectra shown ranged from 7 to 27 ms. The repetition rate of the pulse sequences utilized varied for the complexes from 14 to 32 s^{-1} following the guideline of $1.5T_1$. Accordingly, pulse delays selected were typically less than 100 ms for the low-spin complex and 20–30 ms for the high-spin complexes, including a ~20-ms "recycle delay" inherent to the GE Ω software.[25] All experiments included 32 dummy scans prior to collection of the first block. Generally 512 t_1 blocks were collected with 128–512 scans per block. Total length of time for data collection ranged from 45 min to $3^1/_2$ h. This time actually would have ranged from 24 min to ~2 h except for the recycle delay.[25] Specifics for a given experiment are listed in the figure captions. Spectra shown are collected under optimum conditions for each model compound in terms of sensitivity and detection of all expected cross peaks based on the range of its T_2 values.

Data sets were procssed on a Sun 3/260 workstation using the GE Ω software, version 5.0. The optimal apodization in all cases was determined to be a 0° phase-shifted, sine-bell-squared window, which was applied to a time dimension window closest to $2T_2$ for the peaks of interest. Other apodization functions tried (i.e. sine bell) created more severe peak tailing, obscuring real cross peaks. For complexes with a wide range of T_2 values, care was taken to select the optimal period of the apodization function for each pair of resonances considered. Final 2D data sets are all zero-filled as necessary to 1024 t_2 × 1024 t_1 points prior to Fourier transformation and symmetrization.

Results

Low-Spin (Pyropheophorbidato *a*)iron(III) (1A). The low-spin ferric oxidation/spin state provides the optimal relaxation properties for detecting spin multiplet structure, and 1D spin decoupling has detected[16] all connectivities expected except that for 7H–8H. The 300-MHz NMR trace of **1A** in 2:1 DMSO-$^2H_6$/^2H_2O at 25 °C is illustrated in Figure 1A. The MCOSY map is illustrated in Figure 1B. It reveals all expected cross peaks except the 7H–8H; this, however, is seen in a map recorded on the more sensitive 500-MHz instrument (inset C to Figure 1). The chemical shifts, relaxation properties, and typical J values for resonances expected to exhibit spin coupling are listed in Table I. Thus, all side chains usually assignable by multiplet structure in a diamagnetic complex are similarly assignable in this paramagnetic state.

High-Spin (Protoporphyrinato IX)iron(III) (2). The ^{1}H NMR spectrum of the bis(dimethyl sulfoxide) complex at 80 °C, partially assigned by isotope labeling,[10] is illustrated in Figure 2A, and the

(22) Yu, L. P.; La Mar, G. N.; Rajarathnam, K. *J. Am. Chem. Soc.* **1990**, *112*, 9527.
(23) Bax, A. *Two-Dimensional Nuclear Magnetic Resonance in Liquids*; D. Reidel Publishing Co.: Dordrecht, Holland, 1984.
(24) Bax, A.; Freeman, R.; Morris, G. *J. Magn. Reson.* **1981**, *42*, 164.

(25) We find that an unprogrammed "recycle delay" exists for all pulse sequences in the version 5.0 GE software installed on Ω spectrometers; this recycle delay, which is a programming artifact, was measured to be ~20 ms for the MCOSY sequence. The elimination of the artifact would allow an experiment based on a 20-ms t_2 acquisition time to be collected twice as fast as is presently possible.

Table I. NMR Spectral Data for Spin-Coupled Protons in Ferric Complexes of Pyropheophorbide *a*

		low-spin complex **1A**[b]			high-spin complex **1B**[c]		
proton(s)	J[a]	shift[d]	Δ[e]	T_1[f]	shift[d]	Δ[e]	T_1[f]
$2H_\alpha$	10 ($2H_{\beta c}$), 16 ($2H_{\beta t}$)	42.7	54	35	64.0	130	4.5
$2H_{\beta c}$	10 ($2H_\alpha$), 2 ($2H_{\beta t}$)	−15.7	28	58	−14.0	103	7.8
$2H_{\beta t}$	16 ($2H_\alpha$), 2 ($2H_{\beta c}$)	−14.4	32	100	−19.0	128	4.1
$4C_\alpha H_2$	7 ($4C_\beta H_3$)	−2.9	~40	94	59.0	150	5.2
$4C_\beta H_3$	7 ($4C_\alpha H_2$)	−0.7	~20	125	7.0	130	4.9
$7C_\alpha H_2$	7 ($7C_\beta Hs$), 3 (7H)	−6.0	~30	43	*h*		
$7C_\beta H$	14 ($7C_\beta H'$), 7 ($7C_\alpha Hs$)	−0.8	*g*	42	*h*		
$7C_\beta H'$	14 ($7C_\beta H$), 7 ($7C_\alpha Hs$)	−2.5	40	22	*h*		
7H	2 (8H), 3 ($7C_\alpha Hs$)	24.4	32	38	94.2	240	1.8
8H	2 ($8CH_3$), 2 (7H)	27.6	39	26	74.2	220	2.2
$8CH_3$	2 (8H)	−4.5	16	40	18.2	250	1.5
γCH	17 (γ-CH′)	2.2	~30	28	*h*		
γCH′	17 (γ-CH)	1.6	~30	46	*h*		

[a] Typical coupling constants, in Hz, to proton(s) identified in parentheses. [b] Bis(cyano) complex in 2:1 DMSO-$^2H_6$/^2H_2O. [c] Bis(dimethyl sulfoxide) complex in DMSO-$^2H_6$. [d] Shift at 25 °C in ppm from TMS. [e] Line width, in Hz; uncertainty ±15%. [f] T_1, in ms, for resolved resonances; uncertainty ±15%. [g] Overlap precludes line width determination. [h] Not detected; under intense solvent resonances.

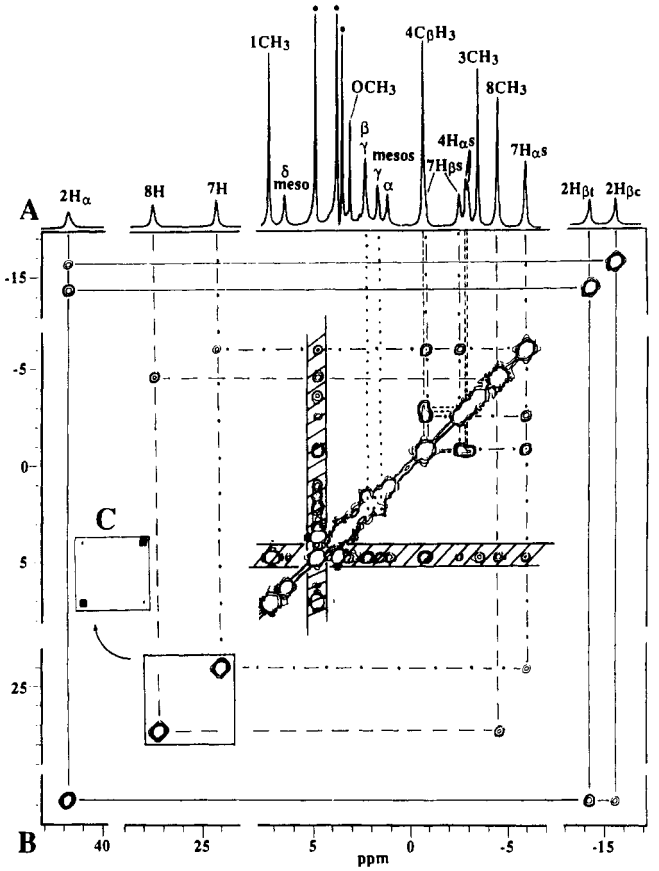

Figure 1. (A) 300-MHz ^1H NMR spectrum of low-spin bis(cyano)(pyropheophorbidato *a*)iron(III) (**1A**) in 2:1 DMSO-$^2H_6$/^2H_2O at 25 °C with peaks labeled as assigned previously.[16] The $5CH_3$ peak was folded-in to improve digitization; impurities and solvent lines are marked ●. (B) 300-MHz symmetrized MCOSY map illustrating cross peaks between spin-coupled resonances. The composite cross peaks involving $4H_\alpha$s, $4C_\beta H_3$, $7H_\beta$s, and $7H_\alpha$s are resolved at 500 MHz (not shown). Data consisted of collecting 512 t_1 blocks with 256 scans of 512 t_2 points each over a bandwidth of 30 kHz (acquisition times of 17 ms in both dimensions). The presented optimal map resulted from apodization over 512 t_1 and 512 t_2 points prior to zero-filling for a final digitization of 29 Hz/point. The 7H–8H cross peak is too weak at 300 MHz but is detected on a more sensitive 500-MHz instrument (inset C). Artifacts from the intense solvent lines are shaded.

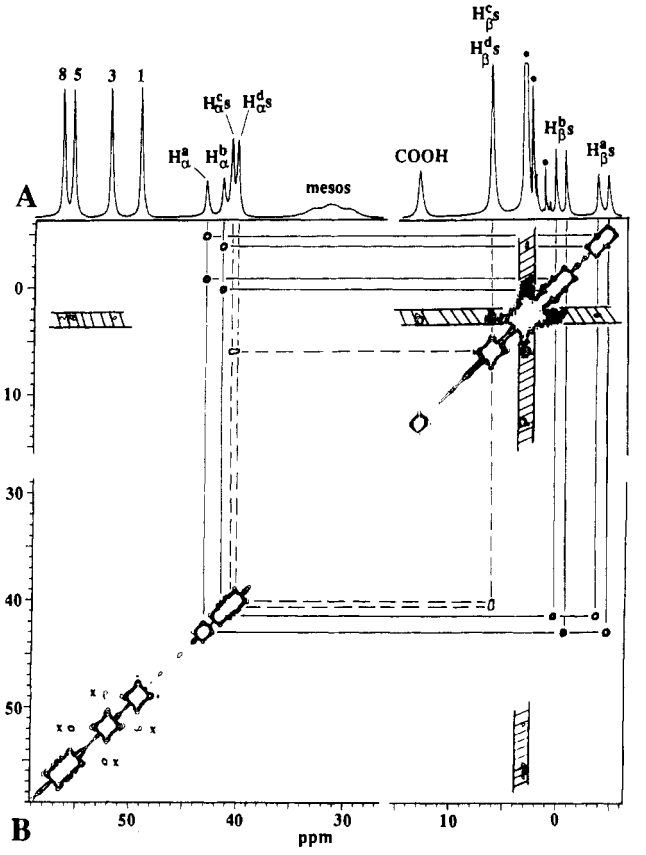

Figure 2. (A) 300-MHz ^1H NMR spectrum of high-spin bis(dimethyl sulfoxide)(protoporphyrinato IX)iron(III) (**2**) in DMSO-$^2H_6$ at 80 °C. The peaks are labeled by collective functional groups (except methyls), as established earlier by deuteration;[10] solvent and impurity lines are marked ●. (B) 300-MHz symmetrized MCOSY map of **2** at 80 °C illustrating cross peaks for the pairs of vinyl and propionate groups; the same cross peaks are also observed at 25 °C. The collected data consisted of 1024 t_1 blocks of 128 scans with 1024 t_2 points over a 45-kHz bandwidth corresponding to acquisition time 22 ms in both dimensions. The presented optimal map resulted from apodizing over 512 t_1 and 512 t_2 points to yield a final digitization of 44 Hz/point. The apparent cross peaks marked x arise from the crossing of the tails or ridges of the intense methyl peaks.[23,24] Similar artifacts due to the solvent lines are indicated by shading.

MCOSY map is given in Figure 2B. While vinyl and propionate H_αs and H_βs have been collectively identified,[10] the H_α and H_β resonances for a given group have not been connected. The MCOSY map clearly reveals two sets of cross peaks between the two low-field and four high-field vinyl protons that identify individual vinyls; the slightly more intense upfield cross peaks, in spite of larger line width, must arise from $H_{\beta t}$ due to the larger J (~16 Hz) than for $H_{\beta c}$ (~10 Hz).[26] Moreover, the two low-field propionate H_α signals yield cross peaks (resolution more clearly seen at higher contour) to the propionate H_βs at 6 ppm.

(26) Scheer, H.; Katz, J. J. In *Porphyrins and Metalloporphyrins*; Smith, K. M., Eds.; Elsevier: Amsterdam, 1975; Chapter 10.

Table II. NMR Spectral Data for Spin-Coupled Protons of High-Spin Bis(dimethyl sulfoxide)(protoporphyrinato IX)iron(III)[a]

proton(s)		J[b]	shift[c]	Δ[d]	T_1[e]
2 or 4	H^a_α	16 ($H_{\beta t}$), 10 ($H_{\beta c}$)	43.0 (47.7)	84 (>100)	6.0
	$H^a_{\beta c}$	10 (H_α), 2 ($H_{\beta t}$)	−0.8 (0.0)	42 (56)	11.2
	$H^a_{\beta t}$	16 (H_α), 2 ($H_{\beta c}$)	−4.8 (−5.4)	75 (89)	4.9
4 or 2	H^b_α	16 ($H_{\beta t}$), 10 ($H_{\beta c}$)	41.4 (~46)	81 (>100)	5.9
	$H^b_{\beta c}$	10 (H_α), 2 ($H_{\beta t}$)	0.2 (−1.2)	42 (58)	12.1
	$H^b_{\beta t}$	16 (H_α), 2 ($H_{\beta c}$)	−3.8 (−6.6)	71 (92)	4.9
6 or 7	$C_\alpha H_2$[c]	7 ($C_\beta Hs$)	40.7 (~46)	88 (>100)	4.9
	$C_\beta H_2$[c]	7 ($C_\alpha Hs$)	6.0 (7.0)	*f*	4.4
7 or 6	$C_\alpha H_2$[d]	7 ($C_\beta Hs$)	40.1 (~46)	85 (>100)	4.8
	$C_\beta H_2$[d]	7 ($C_\alpha Hs$)	6.0 (7.0)	*f*	4.4

[a] In DMSO-$^2H_6$ solvent. [b] Typical spin couplings, in Hz, to proton(s) identified in parentheses. [c] Chemical shifts, in ppm from TMS, at 80 °C (shifts at 25 °C given in parentheses). [d] Line width, in Hz, at 80 °C (line width at 25 °C given in parentheses); uncertainty ±15%. [e] T_1s, in ms, at 80 °C; uncertainty ±15%. [f] Overlap precludes line width determination.

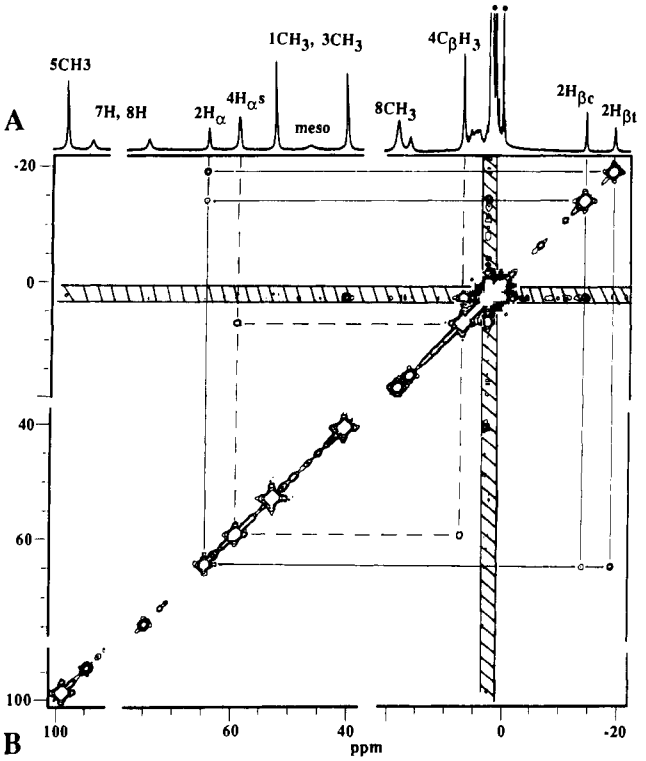

Figure 3. (A) Relevant portions of the 300-MHz ^1H NMR spectrum of the high-spin bis(dimethyl sulfoxide) complex of (pyropheophorbidato *a*)iron(III) (**1B**) in DMSO-$^2H_6$ at 25 °C. Peaks are labeled as determined by isotope labeling or proposed previously[16] and confirmed by present 2D data; solvent and impurity lines are marked ●. (B) 300-MHz MCOSY map of **1B** illustrating cross peaks for the 2-vinyl and 4-ethyl groups. Artifacts from the intense solvent lines are shaded. The data collected consisted of 512 t_1 blocks of 512 scans each with 512 t_2 points over a 68-kHz bandwidth corresponding to acquisition times of 7.4 ms in both dimensions. The presented data were apodized over the collected 512 × 512 points and zero-filled to yield a final digitization of 66 Hz/point. Increasing the number of scans to 3200 per block did not allow detection of cross peaks to either 7H or 8H or between them (not shown).

The chemical shifts and line widths at 25 and 80 °C, as well as typical coupling constants for protons expected to exhibit spin–spin coupling, are listed in Table II. The same six cross peaks observed in Figure 2B at 80 °C are also detected at 25 °C where the lines are much broader (Table II), except that the resolution between the two propionate α-CH_2 signals is lost at the lower temperature (not shown). The only expected cross peak that is not observed is the one between the vinyl H_βs. The small *J* (~2 Hz) is the probable cause.

High-Spin (Pyropheophorbidato *a*)iron(III) (1B). The ^1H NMR trace of the bis(dimethyl sulfoxide) complex reported[16] previously is reproduced in Figure 3A. The chemical shifts and line widths, together with typical spin-coupling constants[26] for protons expected to experience spin–spin coupling, are included in Table I. Earlier work had identified the $5CH_3$ and δ-meso-H by deuteration,[16] and line width considerations had suggested that the peaks at 64.0 and 59.0 ppm arise from the vinyl H_α and $4C_\alpha H_2$. The MCOSY map in Figure 3B clearly reveals two cross peaks from the peak at 64.0 ppm to peaks at −14.0 and −19.0 ppm in the upfield region, establishing their origin as the 2-vinyl H_α, $2H_{\beta c}$, and $2H_{\beta t}$, respectively; $H_{\beta t}$ is distinguished from $H_{\beta c}$ by the more intense cross peak for the former. Moreover, the cross peak between the peak at 59.0 ppm and the methyl signal at 7.0 ppm uniquely identifies the $C_\alpha H_2$ and $C_\beta H_3$ signals of the 4-ethyl group. The propionate signals, as well as those of the γ-meso-CH_2, are insufficiently resolved from each other or the diamagnetic solvent lines[16] to allow detection of the expected cross peaks. The identifications of $2H_\alpha$ and $4C_\alpha H_2$ establish that the pair of peaks at 94.2 and 74.2 ppm must originate from 7H, 8H. However, the failure to detect cross peaks from either of these two peaks to expected spin-coupled signals near the diamagnetic region precludes differentiation between 7H and 8H.

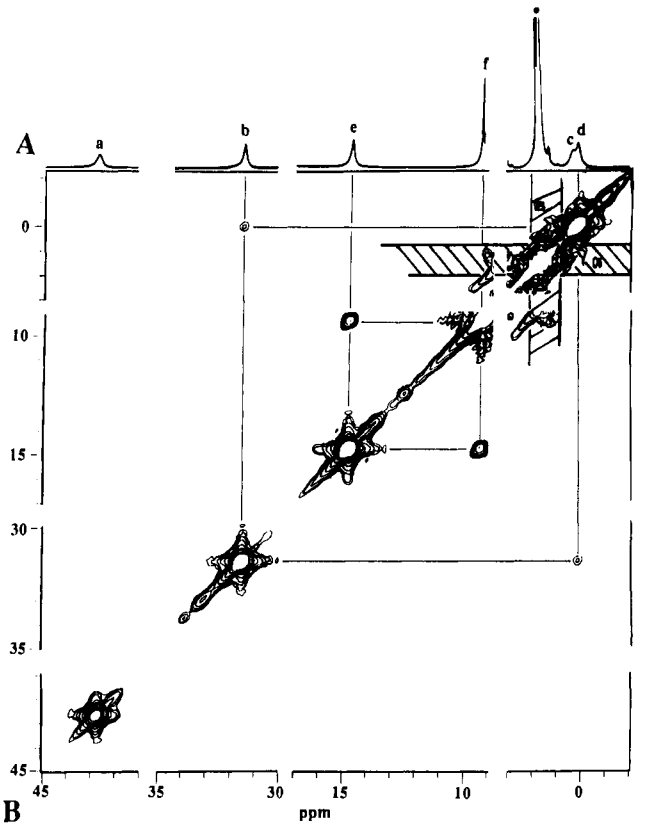

Figure 4. (A) Relevant portions of the 500-MHz ^1H NMR spectrum of high-spin (*N*-methyl tetraphenylporphyrinato)iron(II) chloride (**3**) in C^2HCl_3 at 16 °C, which resolves all four pyrrole-H signals previously collectively identified by deuteration.[9] Solvent and impurity lines are marked ●. (B) 500-MHz MCOSY map illustrating that, of the four pyrrole peaks a–d, only peaks b and d exhibit a cross peak. The cross peak involving peaks e and f entails a phenyl ring *o*-H to *m*-H coupling. Artifacts resulting from the intense solvent lines are shaded. The collected data consisted of 512 t_1 blocks of 128 scans each with 1024 t_2 points over a bandwidth of 50 kHz to yield t_1 and t_2 acquisition times of 10 and 20 ms, respectively. The optimum map resulted from apodization over 512 × 512 points prior to zero-filling in t_1 to yield a final digitization of 49 Hz/point.

High-Spin (*N*-Methyltetraphenylporphyrinato)iron(II) Chloride (3). The sections of interest of the previously reported[9] ^1H NMR spectrum of **3** in C^2HCl_3 at 16 °C are illustrated in Figure 4A. At this temperature the four signals a–d (line width 80–140 Hz) are resolved that arise from the four unique pyrrole Hs (as previously established by selective deuteration[9]) due to the 2-fold symmetry through the methylated pyrrole. The other resolved signals (e, f) arise from the meso-phenyl rings and are not relevant

Table III. NMR Spectral Data for High-Spin (*N*-Methyloctaethylporphyrinato)iron(II) Chloride[a]

	ethyl 1			ethyl 2			ethyl 3			ethyl 4		
	peak	shift[b]	Δ[c]	peak	shift[b]	Δ[c]	peak	shift[b]	Δ[c]	peak	shift[b]	Δ[c]
$C_\alpha H$	a	31.0	71	b	26.6	54	c	23.0	64	g	10.8	56
$C_\alpha H'$	e	16.6	69	f	15.7	55	d	21.0	61	h	5.5	80
$C_\beta H_3$	i	7.5	66	k	1.5	98	j	5.6	45	m	0.2	40
av $C_\alpha H$[d]		23.8			21.2			22.0			8.2	

[a] Data at 15 °C in C^2HCl_3 solvent. [b] Shifts in ppm from TMS. [c] Line width in Hz; uncertainty ±15%. [d] Mean of the two $C_\alpha H$ shifts.

here. The MCOSY map of **3** in Figure 4B clearly reveals only a single cross peak (between peaks b and d) among the four pyrrole-H signals. That cross peak establishes that b and d arise from the protons labeled x and y in **3** on the pyrrole cis to the N-methylated pyrrole (expected coupling[26] ~5 Hz), inasmuch as other coupled pyrrole Hs are equivalent by symmetry. The chemical shifts are listed in Table III. The cross peak for resonances e and f is due to a phenyl ring *o*-H to *m*-H coupling; further analysis of the crowded region 0–10 ppm should allow complete identification of the phenyl resonances; this aspect, however, will be pursued later.

High-Spin (*N*-Methyloctaethylporphyrinato)iron(II) Chloride (4). The trace of **4** in C^2HCl_3 at 15 °C is illustrated in A of Figure 5; the shifts at 25 °C are identical with those reported previously,[9] but resolution is improved at 15 °C. The eight single proton signals a–h have been previously identified as arising from the diastereotopic methylene protons of the four nonequivalent ethyl groups (see **4**), and the four signals i–m as arising from the four attached methyl groups. Expected couplings are only within an ethyl substituent and are ~14 Hz for the geminal and ~7 Hz for the vicinal protons.[26] The MCOSY map for **4** shown in Figure 5B clearly connects the eight protons into four pairs, as well as connecting each of the coupled methylene proton pairs to a methyl group, and identifies the four nonequivalent ethyl groups 1–4 as signals (a, e, i), (b, f, k), (c, d, j), and (g, h, m). The chemical shifts and line widths are listed in Table III.

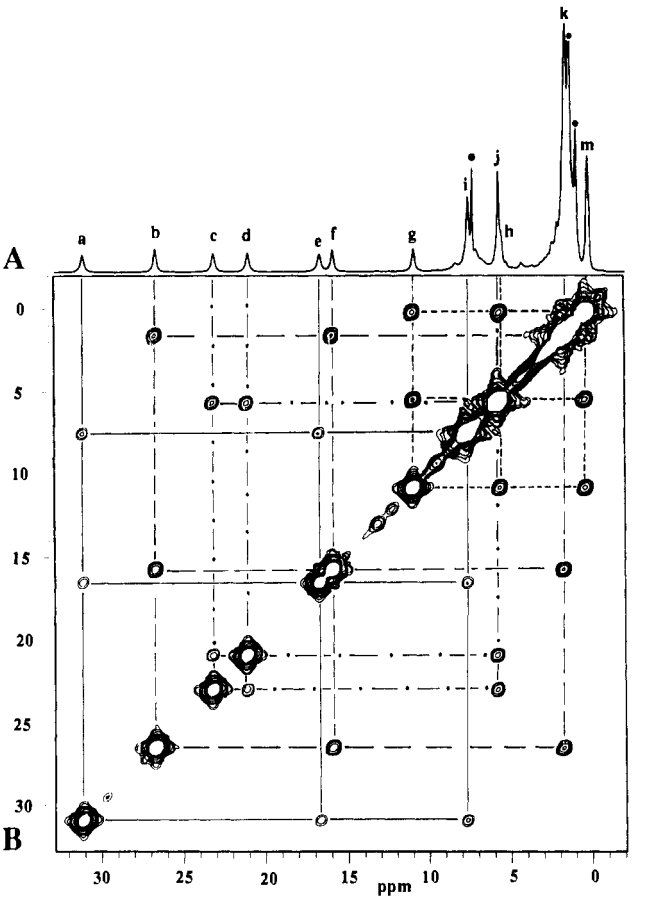

Figure 5. (A) 300-MHz ^1H NMR spectrum of high-spin (*N*-methyloctaethylporphyrinato)iron(II) chloride (**4**) in C^2HCl_3 at 15 °C. Impurity and solvent peaks are labeled ●. (B) 300-MHz MCOSY map of **4** illustrating cross peaks connecting the three signals of the four nonequivalent ethyl groups. Artifacts from solvent lines are shaded. The collected data consisted of 512 t_1 blocks of 128 scans each with 1024 t_2 points over a 50-kHz bandwidth for acquisition times in t_1 and t_2 of 10 and 20 ms, respectively. The optimal map resulted from apodizing over 512 × 512 points prior to zero-filling in t_1 for a final digitization of 49 Hz/point.

Discussion

The 2D MCOSY data in Figures 1–5 clearly show that coherence is detectable in paramagnetic iron complexes of a variety of tetrapyrroles and that such coherence can be detected in the most challenging high-spin ferric and ferrous complexes with broad lines, as well as in the simple, low-spin ferric complexes. In the latter complex, essentially all spin connectivities were detected that could be expected for an analogous diamagnetic system.[26] It is now clear that such MCOSY maps, together with NOESY spectra collected in viscous solvents,[14] should allow unambiguous structure determination of low-spin ferric tetrapyrrole complexes in a manner now applied only to diamagnetic systems. For the high-spin systems, coherence is detected for resonances with coupling constants[26] >7 Hz in spite of line widths as large as 150 Hz. The absence of cross peaks from the more weakly coupled protons (i.e. 7H to 8H) in the high-spin (**1B**) but not low-spin (**1A**) complex is clearly due to the larger line widths (200 Hz vs 50 Hz) in the former, which decreases[21,22] the cross-peak intensity (second term in eq 1) by e^{-4} (~0.02). In addition, the antiphase cancellation will be more severe in the high-spin than low-spin complex because line widths increase for a fixed *J*. However, the observed cross peaks in the high-spin ferric complexes in each case yield valuable assignments that were not obtainable by other means.

In spite of the large spectral width needed (30–68 kHz at 300 MHz), the coherence from the rapidly relaxing signals (T_2s < 7 ms, T_1s < 5 ms) can be effectively encoded with relatively few data points. Although the results presented here utilize 512 t_1 blocks and 512 or 1024 t_2 data points, as few as 256 t_1 blocks and 256 t_2 points produce acceptable results for these complexes (not shown). Hence data collection and storage does not need to exceed that normally utilized for a comparable diamagnetic system. *The shorter T_1s and T_2s of paramagnetic complexes also allow the pulse sequence to be repeated much more rapidly than for a diamagnetic system.* Moreover, as lines become broader and T_1s shorten (i.e. high-spin iron(III)) so that cross peaks will be weaker due to both antiphase cancellation and decay of coherence, the pulse sequence can be repeated both in a more rapid fashion and with a larger number of scans with even fewer t_1 blocks. This much more rapid data acquisition can largely compensate for the inherently weaker cross peaks.

It is obvious that 2D bond correlation experiments have considerable utility, and it can be expected that these 2D experiments will provide many of the needed assignments not only for heme derivatives but for paramagnetic molecules in general. Moreover, MCOSY not only appears to offer the most effective 2D experiment for detection of the bond correlation cross peaks among rapidly relaxing protons but is also the easiest experiment to implement and is readily accessible on relatively unsophisticated modern NMR spectrometers. The MCOSY experiment is even more advantageously implemented for paramagnetic model compounds than for intact hemoproteins,[22] because the broad diagonal that results from the phase-twist line shape[20,21,23,24] is minimized

in models and thereby allows detection of cross peaks close to the diagonal. Conversely, the tailings or ridges that result from the phase-twist line shape even under optimal processing conditions can lead to artifacts in the form of apparent cross peaks due simply to the crossing of the ridges from two intense peaks[23,24] (i.e., see apparent cross peaks marked x in Figure 2B). Problems with such apparent cross peaks can be avoided by interpreting only cross peaks whose intensity significantly exceeds that predicted by the sum of the respective ridges. Alternative routes to circumventing the antiphase cancellation of broad peaks are based on the pure absorption cross peaks of the TOCSY experiment.[27,28] However, we find that the substantial pulse power needed to spin-lock over large spectral widths, together with the lengthy mixing times required to develop coherence during which the magnetization of interest decays, severely limits the general utility of this experiment for strongly relaxed lines.[22]

Perhaps the most unique and intriguing prospect for COSY applications in paramagnetic iron tetrapyrrole complexes is the characterization of asymmetric peripheral perturbations on the molecular orbitals of the tetrapyrrole, as reflected in the unpaired spin distribution. Thus the pseudo-4-fold symmetry of a porphyrin can be disrupted via reduction of a pyrrole to yield a chlorin[15,16] (i.e., complex **1**), insertion of a ligand into a pyrrole–iron bond (i.e. carbene insertion[9]), or alkylation of a pyrrole nitrogen[9] (i.e. complexes **3** and **4**). With respect to the N-alkylated ferrous porphyrins, one of the questions that arises is whether the asymmetric spin density reflected in the large spread of the pyrrole (or methylene proton) substituent signals reflects solely asymmetry among the different types of pyrroles or is there large asymmetry even within a pyrrole? Similar questions arise with respect to the large spread of signals in octaethylchlorins.[29] As the data in Figure 4 clearly show for (*N*-methyltetraphenylporphyrinato)-iron(II) (**3**), one pyrrole (likely protons z on the pyrrole trans to the N-alkylated pyrrole of **3**) has large spin density (peak a), one pyrrole (likely protons w on the N-alkylated pyrrole in **3**) has very little spin density (peak c), but the two pyrroles cis to the alkylated pyrrole exhibit a marked asymmetry within that pyrrole ring; one of the protons reflects a large spin density (peak b), while the other one indicates essentially none (peak d). Assignment of the peaks b and d to individual protons x and y in **3** is not yet possible. A slightly different asymmetry is reflected in the α-methylene protons of **4**, where the mean α-CH_2 shift (Table III) is distinctly smaller for only one of the four α-CH_2 groups (peaks g, h, m). The nature of the delocalized spin density and identity of the molecular orbital(s) in which it resides[1-6] could be determined if the contact shifts of the pyrrole H and α-CH_2 could be correlated. The present studies clearly show that the first step in the critical assignments needed to elucidate the electronic structure in this class of paramagnetic complexes, as well as others, is readily accessible by modern 2D NMR methods. The next step will be to implement NOESY studies in viscous solvents[14,16] to establish the spatial proximity of noncoupled groups. A search for a viscous solvent chemically compatible with the systems of interest is in progress.

Acknowledgment. We thank and are indebted to Drs. M. Renner and C. R. Cornman for experimental assistance. This research was supported by grants from the National Institutes of Health, GM 26226, HL 16087, and HL 22252. The GE NMR Ω-300 and Ω-500 spectrometers were purchased in part with funds from the National Science Foundation, Grants BBS-88-04739 and DIR-90-16484, and the National Institutes of Health, Grant RR-04795.

(27) Braunschweiler, L.; Ernst, R. R. *J. Magn. Reson.* **1983**, *53*, 521. Bax, A.; Davies, D. G. *J. Magn. Reson.* **1985**, *65*, 355.
(28) Luchinat, C.; Steuernagel, S.; Turano, P. *Inorg. Chem.* **1990**, *29*, 4351.
(29) Pawlik, M. J.; Miller, P. K.; Sullivan, E. P., Jr.; Levstik, M. A.; Almond, D. A.; Strauss, S. H. *J. Am. Chem. Soc.* **1988**, *110*, 3007.

Contribution from the Department of Chemistry, Gorlaeus Laboratories, Leiden University, P.O. Box 9502, 2300 RA Leiden, The Netherlands, and School of Chemical Sciences, Dublin City University, Dublin 9, Ireland

Mononuclear and Dinuclear Ruthenium Complexes with Triazole-Containing Ligands: Fine-Tuning of the Spectroscopic Properties

Ronald Hage,[†] Jaap G. Haasnoot,*[,†] Jan Reedijk,[†] Renyi Wang,[‡] and Johannes G. Vos[‡]

Received September 25, 1990

The synthesis, characterization and properties of mononuclear and dinuclear $Ru(bpy)_2$ complexes with $bpzt^-$ and $mbpt^-$ are reported (bpy = 2,2′-bipyridine, Hbpzt = 3,5-bis(pyrazin-2-yl)-1,2,4-triazole, and Hmbpt = 3-(6-methylpyridin-2-yl)-5-(pyridin-2-yl)-1,2,4-triazole). Both ligands deprotonate easily upon coordination to the $Ru(bpy)_2$ moiety. The coordination mode of the complexes was determined by using ^1H NMR spectroscopy. For the mononuclear compounds, $[Ru(bpy)_2(L)]^+$, only coordination via N1 of the triazole ring and the pyridine or pyrazine nitrogen takes place. The two ruthenium centers in the dinuclear compounds with $mbpt^-$ and $bpzt^-$ are bound via N1 and N4 of the triazole ring. Electrochemical and resonance Raman measurements indicate that for $[(Ru(bpy)_2)_2(bpzt)]^{3+}$ and $[Ru(bpy)_2(Hbpzt)]^{2+}$ the first reduction potential is $bpzt^-$ based. $[Ru(bpy)_2(bpzt)]^+$, $[Ru(bpy)_2(mbpt)]^+$, and $[(Ru(bpy)_2)_2(mbpt)]^{3+}$ exhibit a bpy-based reduction. This suggests that in the dinuclear $bpzt^-$ compound and in the protonated compound, the π^* level of the $bpzt^-$ ligand is lower than that of the bpy ligand, while the LUMO (lowest unoccupied molecular orbital) is located on the bpy ligand in $[Ru(bpy)_2(bpzt)]^+$. The mixed-valence complexes $[(Ru(bpy)_2)_2(bpzt)]^{4+}$ and $[(Ru(bpy)_2)_2(mbpt)]^{4+}$ exhibit intervalence-transition bands at 5400 cm^{-1} (ϵ = 2200 M^{-1} cm^{-1}) and 5400 cm^{-1} (ϵ = 2400 M^{-1} cm^{-1}), respectively. The extent of electron delocalization is in both cases quite high (α^2 = 0.019 and 0.020 respectively), suggesting a fairly strong metal–metal interaction via the HOMO (highest occupied molecular orbital) of the triazolate bridge.

Introduction

Considerable attention has been paid to dinuclear ruthenium systems, not only because of their potential as two-electron-transfer intermediates in water-splitting devices[1] but also because of the general interest in the physical properties of redox-active dinuclear compounds.[2-16] After partial oxidation of such dinuclear species, mixed-valence species can be obtained, which can yield information about electron delocalization and the degree of metal–metal in-

(1) (a) Seddon, E. A.; Seddon, K. R. *The Chemistry of Ruthenium*; Elsevier Science Publishers BV: Amsterdam, 1984. (b) Meyer, T. J. *Pure Appl. Chem.* **1986**, *58*, 1193. (c) Kalyanasanduram, K.; Grätzel, M.; Pelizzetti, E. *Coord. Chem. Rev.* **1986**, *69*, 57.
(2) (a) Geselowitz, D. A.; Kutner, W.; Meyer, T. J. *Inorg. Chem.* **1986**, *25*, 2015. (b) Gilbert, J. A.; Eggleston, D. S.; Murphy, W. R.; Geselowitz, D. A.; Gersten, S. W.; Hodgson, D. J.; Meyer, T. J. *J. Am. Chem. Soc.* **1985**, *107*, 3855. (c) Vining, W. J.; Meyer, T. J. *Inorg. Chem.* **1986**, *25*, 2023.

[†] Leiden University.
[‡] Dublin City University.

0020-1669/91/1330-3263$02.50/0